

ORIGINAL ARTICLE

Chromatic and Achromatic Spatial Resolution of Local Field Potentials in Awake Cortex

Michael Jansen¹, Xiaobing Li¹, Reza Lashgari^{1,4}, Jens Kremkow¹, Yulia Bereshpolova³, Harvey A. Swadlow^{1,3}, Qasim Zaidi², and Jose-Manuel Alonso^{1,3}

¹Department of Biological Sciences and ²Graduate Center for Vision Research, SUNY College of Optometry, New York, NY, USA, ³Psychology, University of Connecticut, Storrs, CT, USA, and ⁴Department of Biomedical Engineering, School of Electrical Engineering, Iran University of Science and Technology, Tehran, Iran

Address correspondence to Jose-Manuel Alonso, State University of New York, State College of Optometry, 33 West, 42nd street, 17th floor, New York, NY 10036, USA. Email: jalonso@sunyopt.edu

Abstract

Local field potentials (LFPs) have become an important measure of neuronal population activity in the brain and could provide robust signals to guide the implant of visual cortical prosthesis in the future. However, it remains unclear whether LFPs can detect weak cortical responses (e.g., cortical responses to equiluminant color) and whether they have enough visual spatial resolution to distinguish different chromatic and achromatic stimulus patterns. By recording from awake behaving macaques in primary visual cortex, here we demonstrate that LFPs respond robustly to pure chromatic stimuli and exhibit ~2.5 times lower spatial resolution for chromatic than achromatic stimulus patterns, a value that resembles the ratio of achromatic/chromatic resolution measured with psychophysical experiments in humans. We also show that, although the spatial resolution of LFP decays with visual eccentricity as is also the case for single neurons, LFPs have higher spatial resolution and show weaker response suppression to low spatial frequencies than spiking multiunit activity. These results indicate that LFP recordings are an excellent approach to measure spatial resolution from local populations of neurons in visual cortex including those responsive to color.

Key words: LFP, area V1, color, receptive field, striate cortex

Introduction

The primary visual cortex (area V1) is fed by 3 major thalamic pathways that carry different combinations of inputs from cone photoreceptors that are sensitive to long (L), medium (M), and short (S) wavelengths. Parvocellular neurons compute the difference between L and M inputs, koniocellular neurons the difference between S and the sum of L + M inputs, and magnocellular neurons compute L + M sums (Derrington et al. 1984; Sun et al. 2006). Magnocellular and parvocellular neurons measure local

contrast by taking the difference between inputs to their receptive field centers and surrounds (Wiesel and Hubel 1966; Reid and Shapley 1992, 2002; Lee et al. 1998). When the center and surround involve the same cone combination, the subtraction generates band-pass spatial frequency tuning, as is the case in magnocellular neurons, where only a band of intermediate spatial frequencies pass to later stages of visual processing (Hicks et al. 1983; Derrington and Lennie 1984). Conversely, when the center-surround subtraction involves different cones, as in the parvocellular pathway, the neurons only pass the low spatial

frequencies of equiluminant red/green gratings (low-pass tuning). Since koniocellular neurons subtract ($L + M$) from S , they also pass only the low spatial frequencies of equiluminant blue/yellow gratings (Szmajda et al. 2006; Tailby, Solomon, et al. 2008; Tailby, Szmajda, et al. 2008; Roy et al. 2009).

The sensitivity of humans to different spatial frequencies matches the sensitivity of thalamic and retinal ganglion cells measured in macaque monkeys. Like thalamic neurons, the human spatial frequency tuning is low-pass for chromatic gratings and band-pass for achromatic gratings and the visual acuity is also 3 times higher for achromatic than chromatic gratings [~ 30 vs. 10 cycles/ $^\circ$ (Mullen 1985)]. However, while the chromatic spatial frequency tuning is low-pass in humans, it can be low-pass or band-pass in single cortical neurons (Thorell et al. 1984; Lennie et al. 1990; Leventhal et al. 1995; Johnson et al. 2001, 2004, 2008). Therefore, human perception at threshold does not match the sensitivity of individual cortical neurons and finding a better match may require measurements of combined activity from neuronal populations. Our current understanding of neuronal population responses to color relies on measurements made on single neurons or functional magnetic resonance imaging (fMRI). Another measure of neuronal population activity, the local field potential (LFP), has received renewed interest in recent years because of its potential use for cortical prosthesis (Andersen et al. 2004). However, it remains unclear whether LFPs can generate robust responses to equiluminant chromatic gratings and have enough spatial resolution to resolve different chromatic and achromatic stimulus patterns. Here, we demonstrate that LFPs recorded through the depth of the cortex respond robustly to chromatic equiluminant gratings and, similar to human perception, LFP responses have lower spatial resolution and are more low-pass for chromatic than achromatic gratings. In addition, we demonstrate that LFP responses have higher spatial resolution and weaker size suppression than multiunit activity. Therefore, we conclude that LFP signals provide an excellent measure of local V1 activity and have better spatial resolution than multiunit spiking activity.

Materials and Methods

Surgery and Preparation

Two adult male rhesus monkeys were surgically implanted with a head post, a scleral eye coil, and a recording chamber. Inside the recording chamber, we implanted a chronic multielectrode array with 3–7 independently movable electrodes to record LFP activity (Swadlow et al. 2005). The electrodes were 40- μm -diameter platinum-tungsten filaments, pulled, and sharpened to a fine tip of ~ 1 μm . Animals were trained to hold a bar and fixate on a small cross of 0.12° . After fixating for 0.5 s, static sine-wave gratings were presented over a period of 2 s to measure the chromatic selectivity, spatial frequency tuning, and size tuning of LFPs. Each trial was aborted and repeated if the animal fixation deviated more than 1° from the center of the cross or if the animal released the bar prior to the end of stimulus presentation. To estimate the cortical depth of the recordings, we measured the polarity of the LFP waveform based on summing the first 60 ms of response following the first presentation of a luminance grating. All procedures were performed in accordance with the guidelines of the US Department of Agriculture and approved by the Institutional Animal Care and Use Committee at the State University of New York, College of Optometry [see (Chen et al. 2008) for further details].

Visual Stimuli

Stimuli were presented on a cathode ray tube (CRT) monitor (Sony GDM F520, refresh rate: 160 Hz). The receptive field of the LFP was mapped with sparse noise consisting of either 256 light squares presented on a 16×16 grid ($0.71^\circ/\text{square}$ side) or 1600 light squares presented on a 40×40 grid ($0.59^\circ/\text{square}$ side). Light squares were flashed for 20 ms and separated by 100 ms. When a single neuron was recorded simultaneously with the LFP, the grating stimulus was centered at the receptive field position of the neuron. In these cases, the receptive field center of each single neuron was mapped using the spike-triggered average of Hartley stimuli (Ringach et al. 1997) presented at 80 Hz. The Hartley stimuli were made of gratings with 88 different orientations, 41 different spatial frequencies, and 4 different phases, usually presented at 2–3 different sizes (0.1, 0.2, and 0.4° per pixel). In LFP recordings, the spatial frequency tuning was measured with large grating stimuli of 8° diameter and 0° orientation. We chose these stimulus parameters because equiluminant chromatic gratings generated the most robust LFP response transients to large gratings (see Results for size tuning in this article) and the amplitude of the LFP transient was poorly tuned to orientation (Lashgari et al. 2012). LFPs are also untuned to orientation when flashed bars are used (Mineault et al. 2013).

The emission spectra for the red (R), green (G), and blue (B) monitor phosphors were measured with a Photo Research PR 650 SpectraScan spectroradiometer. Since our LFP recordings cover foveal receptors, excitations for the long- (L), medium- (M), and short- (S) wavelength sensitive cones were obtained for the 3 phosphors from the dot product of the emission spectra and the Smith–Pokorny 2° cone fundamentals (Smith and Pokorny 1975). Using the procedure described by Zaidi and Halevy (1993), this cone response space was converted to the cardinal color space used by Derrington et al. (1984) defined by ($L - M$), (S), and ($L + M + S$) axes. For simplicity, we will call ($L - M$) the red/green axis (RG), S the blue/yellow axis (BY), and ($L + M + S$) the light/dark or luminance axis (LD). S and ($L + M$) cone absorptions are constant in the RG axis, L and M are constant in the BY axis, and all cone absorptions vary together in the LD axis. Figure 1 shows the L , M , and S coordinates at the intersection and ends of the 3 cardinal axes. Cone contrasts were calculated for each axis as in the following equation:

$$|\Delta L_{\max}/W_L| + |\Delta M_{\max}/W_M| + |\Delta S_{\max}/W_S| \quad (1)$$

where W_L (0.647), W_M (0.353), and W_S (0.0109) are the cone excitations at the white point (W) and ΔL_{\max} , ΔM_{\max} , and ΔS_{\max} are the maximum excursions from the white point to the end of each axis. Notice that cone excitations are dimensionless units as they are calculated as the ratios of cone absorptions (MacLeod and Boynton 1979). ΔL_{\max} , ΔM_{\max} , and ΔS_{\max} are, respectively, 0.647, 0.353, and 0.0109 at the LD axis, 0.036, 0.036, and 0 at the RG axis and 0, 0, and 0.0079 at the BY axis. The W and Δ_{\max} values are used to calculate the cone excitations at each axis edge.

After applying Equation (1), the maximum cone contrasts available along the RG, BY, and LD axes were:

RG : contrast (L) = 5.56%, contrast (M) = 10.1%, contrast (S) = 0%
 BY : contrast (L) = 0%, contrast (M) = 0%, contrast (S) = 72.5%
 LD : contrast (L) = 100%, contrast (M) = 100%, contrast (S) = 100%.

The maximum cone contrast was 4.5 times lower along the RG axis ($5.56 + 10.1\% = 15.7\%$) than along the BY axis (72.5%) because cone excitations are heavily correlated between L and M .

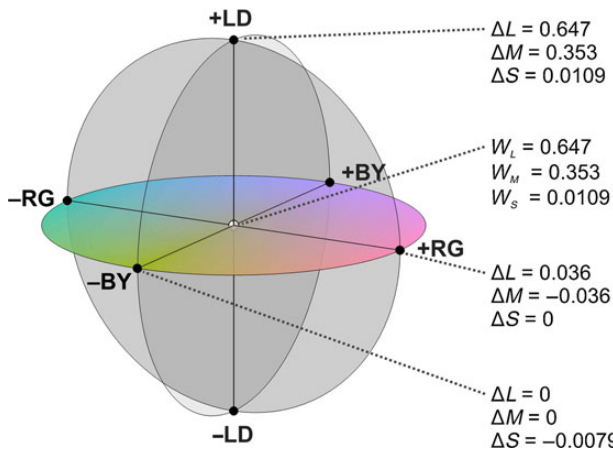


Figure 1. Color space. The equiluminant chromatic plane is defined by the red/green (RG) and blue/yellow (BY) axes while the light/dark (LD) axis is orthogonal to this plane. The red/green axis is calculated as $\Delta(L - M)$, the blue/yellow axis as $\Delta(S - (L + M))$ and the light/dark axis as $\Delta(L + M + S)$, where L , M , and S are the excitations for the 3 different types of cones. W_L , W_M , and W_S are the excitations at the white point for the L , M , and S cones, respectively. Changes in cone excitations for each of the axes are shown.

In these color tests, we did not use the maximum cone contrast available. Instead, the cone contrasts were set to 85% of the maximum to allow adding an LD grating with 15% contrast to RG and BY gratings. This addition was needed to identify LFP chromatic responses with our phase test (see below). Therefore, the maximum cone contrast in the RG axis was 85% of 15.7% (13.3%) and the maximum contrast in the BY axis was 85% of 72.5% (61.6%). Since we were recording LFPs from populations of cells, we chose to manipulate stimuli in a thalamus-based space rather than along cone axes (Shapley and Hawken 2011). The thalamic axes facilitate separation of population chromatic responses from luminance responses, whereas cone axes (e.g., L-cone isolating stimuli) would give a mix of chromatic and luminance responses.

Identification of LFP Chromatic Responses

To identify pure chromatic LFP responses, we selected only those sites that responded stronger to RG and BY gratings than to a 15% contrast LD grating (Fig. 2a–c, contrast test). This approach rejected any LFP chromatic response that could be caused by an artifactual luminance mismatch between the 2 chromatic bars of the grating. Because the maximum cone contrast used in the RG axis was 13.3%, the largest residual luminance possible (13.3%) was lower than the luminance of 15% contrast LD gratings. Luminance mismatches are more likely to be a problem in equiluminant BY gratings because the macular pigment absorbs more blue than yellow light (Snodderly, Brown, et al. 1984). Out of all cases examined by Cottaris (2003), the maximum artifact occurred with S cone isolating stimuli (at 84% cone contrast), which gave a combined L and M cone contrast of 10.8% in the macaque. Since 10.8% is smaller than 15%, an LFP recording site was classified as chromatic if the LFP responded more strongly to BY gratings than 15% LD gratings.

This contrast test was very strict and rejected many LFPs that responded robustly to chromatic contrast but also responded to low luminance contrast. Because combined color/luminance responses are very common in neurons from area V1 (Johnson et al. 2001, 2004), we used a second phase-independence test to

identify LFP chromatic responses. In the phase test, we added a 10–15% LD grating to our luminance and chromatic gratings either in-phase or opposite-phase (Fig. 2d–f; phase test). LFP luminance responses were stronger when the added gratings were in phase with the luminance component than when they were out of phase. If a chromatic grating had only an insignificant luminance component, LFP responses would not differ across phase combinations. Therefore, a robust LFP response was classified as chromatic by the phase test if there was no significant difference between the paired responses of the 4 phase combinations. To discard noisy measurements, the responses to chromatic gratings without luminance component had to have a signal-to-noise ratio (SNR) ≥ 2 (see below for definition of SNR). In total, we measured the responses of 92 different LFP recording sites, which were tested for significant chromatic responses with the contrast test ($n = 80$) and the phase test ($n = 92$). Twenty-five LFP recordings passed the phase test for red/green gratings, 23 for blue/yellow gratings, and 16 for both. Seventeen LFP recordings passed the contrast test for red/green gratings, 20 for blue/yellow gratings, and 16 for both. Of the 80 LFP recordings subjected to both contrast and phase tests, 16 passed both tests, 15 for blue/yellow gratings, 13 for red/green gratings, and 12 for both color axes.

Data Analysis

To measure the spatial frequency tuning and size tuning, static gratings were presented for 20 ms and separated by blanks of 480 ms in a sequence that lasted 2 s. The parameter range was 0.01–6 cycles per degree (cpd) for spatial frequency and 0.5–12° for size tuning. We used a maximum LD axis contrast of 94% for all LFP measurements of spatial frequency tuning and size tuning with the exception of 6 LFP recordings in which the spatial frequency tuning was obtained at a maximum LD axis contrast of 30%.

Both multiunit activity (MUA) and LFP visual responses were measured simultaneously within a temporal window of 250 ms following the stimulus onset, as the average of 32 amplitude values (4 stimulus onsets per trial, 8 trials). The LFP amplitude was defined as the difference between the peak (maximum) and trough (minimum) LFP value within the 250 ms, which is a measure commonly used to characterize the amplitude of histograms, impulse responses, and visual evoked potentials driven by brief stimuli. Notice that the LFP amplitude measured with brief static stimuli (20 ms) is different from the amplitude of LFP frequency components measured with gratings drifting for several seconds (Lashgari et al. 2012). Trials with LFP amplitudes >1 mV were rejected from the analysis to avoid occasional LFP deflections caused by small movements such as licking, which were rare in our recordings. We restricted our analysis to LFP recordings that had enough amplitude to perform reliable measurements. To select robust LFP recordings, we calculated the SNR of the LFP average. The SNR was measured as the maximum LFP amplitude divided by twice the standard deviation of the baseline (500 ms preceding the stimulus onset). We chose this SNR measurement because it relates the noise directly to the LFP amplitude. We chose to measure the standard deviation of the baseline noise because it is a robust measurement based on multiple values and not just 2 arbitrary noise maximum and minimum values. We selected LFP recordings with SNR ≥ 2 measured at the spatial frequency peak for spatial frequency tuning and at the preferred size for size tuning. MUA responses were converted to spike density waveforms ($\sigma = 10$ ms). The SNR for MUA was calculated as the maximum response within the first 250 ms following the

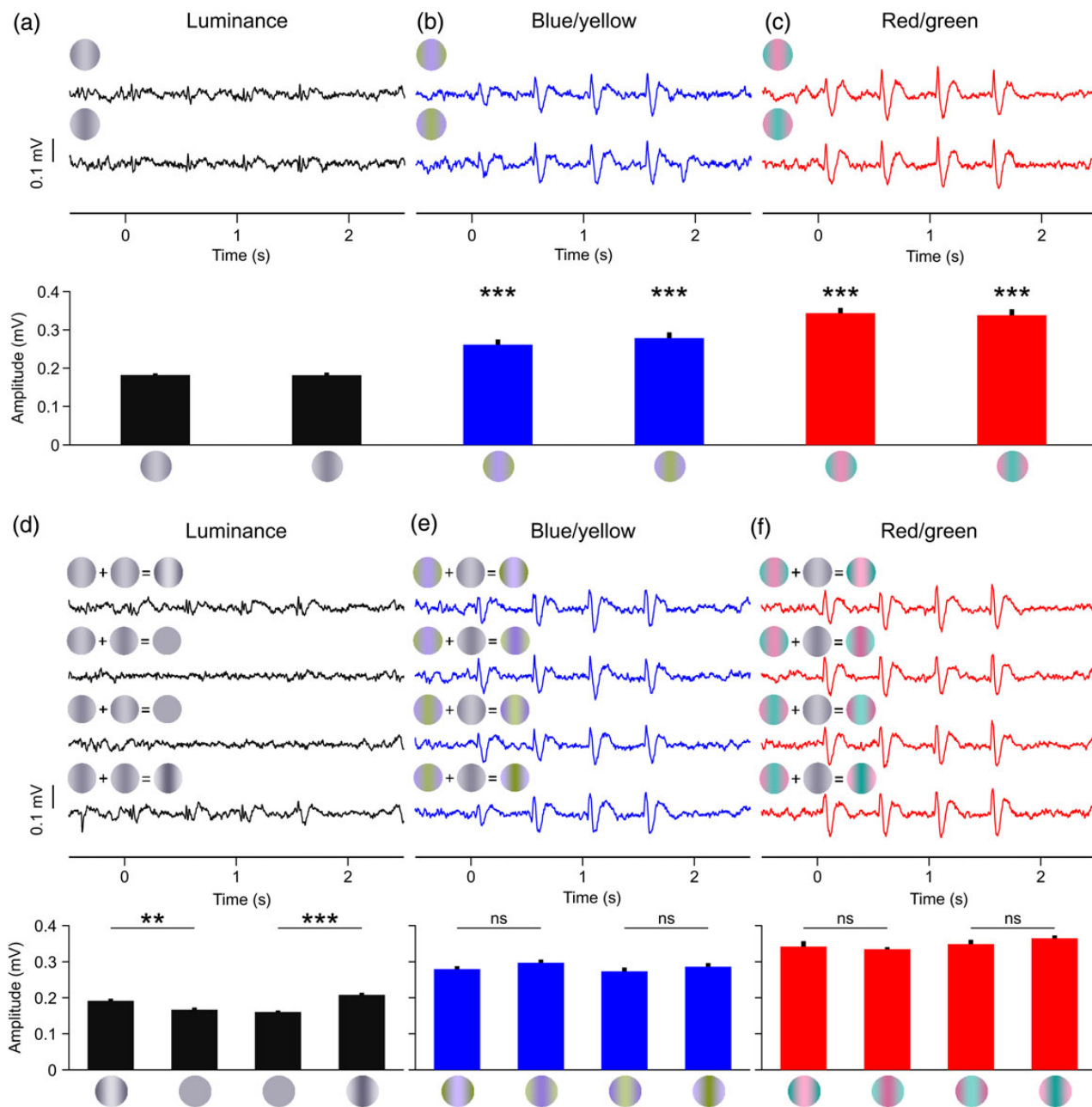


Figure 2. LFP chromatic responses for the contrast test (a–c) and the phase test (d–f). LFP traces (top) and mean LFP amplitude (bottom) for the 3 cardinal axis: luminance (a,d), blue/yellow (b,e), and red/green (c,f). The gratings at the top left corner of the LFP trace illustrate the stimulus phase (a–c) or the phase combination used to construct the stimulus (d–f). See Materials and Methods for details. t-Test: *** $P < 0.001$, ** $P < 0.01$, * $P < 0.05$, ns = not significant, $n = 8$ trials.

stimulus onset minus the average baseline divided by the standard deviation of the baseline. Only MUA with $\text{SNR} \geq 2$ were used for further analysis.

The spatial frequency tuning curves for both LFP and MUA were fit with Gaussian functions and the size tuning curves with a Naka-Rushton (hyperbolic) function. Only fits with $r^2 \geq 0.6$ were used to extract tuning values. From the spatial frequency tuning, we extracted the peak frequency, the high spatial frequency cutoff and the band-pass index. The peak spatial frequency was defined as the peak of the Gaussian. The high spatial frequency cutoff was defined as the spatial frequency higher than the peak that generated half-maximum response. The band-pass index was defined as the ratio of the response at the

peak spatial frequency to the response at the lowest spatial frequency tested (0.01 cpd). The band-pass ratio was 1 for LFPs with low-pass spatial frequency tuning and larger than 1 for those with band-pass tuning. From the size tuning fit of each LFP recording, we extracted the size that generated the maximum responses (peak size), the size that generated 50% of the maximum responses (S50) and the suppression index. The suppression index was defined as 1 minus the ratio between the response to the largest grating tested and the peak response. The suppression index equals 1 if the largest grating suppresses completely the LFP response and 0 if it does not suppress the response.

We measured the LFP spatial frequency tuning in 92 recording sites and 66 passed our criteria for SNR (≥ 2) and tuning fit

($r^2 \geq 0.6$), 43 for luminance gratings, 44 for blue/yellow gratings, and 51 for red/green gratings (note that many LFP recordings were tuned to both luminance and color). Out of the LFP recordings that showed significant tuning to chromatic gratings, 36 passed our chromatic tests (21 for the contrast test, 31 for the phase test, and 16 for both); 28 were tuned to blue/yellow gratings, 27 to red/green gratings, and 19 to both. Of the 92 recording sites, only 29 MUA recordings passed our significance criteria for SNR (≥ 2) and tuning fit ($r^2 \geq 0.6$). Out of the 29 MUA recordings tuned to spatial frequency, 18 were tuned to luminance gratings, 16 to blue/yellow, and 11 to red/green gratings. Eleven MUA recordings were associated with chromatic LFP responses (8 classified based on the contrast test and 9 based on the phase test). From these 11 MUA recordings, 9 responded to blue/yellow gratings and 5 also responded to red/green gratings. In 29 MUA recordings, the spatial frequency tuning was significant for at least one of the 3 cardinal axes (red/green, blue/yellow, or luminance) and, in 21 recordings, it was significant for at least one of the 2 chromatic axis (red/green or blue/yellow).

We measured LFP size tuning in 63 recording sites and 52 passed our criteria for SNR (≥ 2) and tuning fit ($r^2 \geq 0.6$), 50 for luminance gratings, 23 for blue/yellow gratings, and 25 for red/green gratings. From these 52 recordings, 17 passed our chromatic tests (13 for the contrast test, 13 for the phase test, and 9 for both); 14 were tuned to blue/yellow gratings, 12 to red/green gratings, and 9 to both. We measured MUA size tuning in the same 63 recording sites but only 19 MUA recordings passed our significance criteria for SNR (≥ 2) and tuning fit ($r^2 \geq 0.6$). From these 19 MUA recordings with robust size tuning, 15 were tuned to luminance gratings, 9 to blue/yellow gratings, and 9 to red/green gratings. Seven MUA recordings were associated with chromatic LFP responses (5 classified with contrast test and 7 with phase test); 6 responded to blue/yellow gratings; and 2 to red/green gratings (1 responded to both).

Results

We used a chronically implanted multielectrode array with independently movable electrodes to record LFPs in area V1 of awake primates at different cortical depths (Swadlow et al. 2005; Chen et al. 2008). LFP responses to chromatic contrast were identified with 2 different tests: a contrast test ($n = 80$) and/or a phase test ($n = 92$). In the contrast test, an LFP recording site was classified as “chromatic” (responsive to chromatic contrast) if the response to red/green or blue/yellow gratings was significantly stronger than the response to luminance gratings with 15% contrast (Fig. 2a–c; luminance: 0.189 and 0.189 mV, blue/yellow: 0.261 and 0.278 mV, $P < 0.001$; red/green: 0.344 and 0.338 mV, $P < 0.001$, t -tests). Because many V1 cells respond strongly to both equiluminant and luminance gratings (Johnson et al. 2001, 2004), we used the phase independence between luminance and chromaticity to avoid misclassifying a large number of LFP recordings as non-chromatic. In this phase test, we added a luminance grating of 10–15% contrast to a luminance, blue/yellow, or red/green grating. Because the 2 added gratings could have 2 different phases, we generated 4 phase combinations of stimuli in total. By using this approach, LFPs driven by low luminance contrast responded well when the added gratings were in phase (Fig. 2d, top and bottom LFP traces) but not when they were out phase (Fig. 2d, middle LFP traces). On the contrary, LFPs driven by pure chromatic contrast responded equally well to all phase combinations (Fig. 2e,f). As illustrated in Figure 2d–f, this approach identified LFP chromatic responses even if the LFP responded to low luminance contrasts.

Spatial Frequency Tuning

After identifying LFP recording sites that responded to pure chromatic contrast, we measured the spatial frequency tuning of the LFP with luminance (94% or 30% contrast), blue/yellow (94% contrast), and red/green gratings (94% contrast). Figure 3 illustrates 2 examples of LFP recordings classified as chromatic with both red/green and blue/yellow gratings. The LFPs illustrated in Figure 3a–d were recorded at 10.43° eccentricity (azimuth: 9.71°, elevation: 3.82°), and the average response amplitude was larger for luminance (0.60 mV) than blue/yellow (0.45 mV) and red/green (0.37 mV) gratings. The peak of the spatial frequency tuning and spatial frequency cutoff were highest for luminance gratings (peak: 3.53 cpd, cutoff: 6.00 cpd), intermediate for blue/yellow gratings (peak: 0.84 cpd, cutoff: 1.32 cpd) and lowest for red/green gratings (peak: 0.27 cpd, cutoff: 1.06 cpd). The spatial frequency tuning was more band-pass for luminance (2.45) and blue/yellow gratings (2.71) than for red/green gratings (1.05). Unlike Figure 3a–d, the LFPs illustrated in Figure 3e–g were band-pass for all 3 cardinal axes of color space (band-pass ratio: 1.46 for luminance, 1.57 for red/green, and 1.75 for blue/yellow). However, the LFP spatial frequency peak and cutoff were still higher for luminance than chromatic gratings (peak/cutoff: 0.98/1.40 cpd for luminance, 0.82/1.31 cpd for blue/yellow, 0.68/1.22 cpd for red/green), while the LFP amplitudes were similar (0.12 mV for luminance, blue/yellow, and red/green).

Many LFP recordings could not be classified as chromatic with our contrast and phase tests. In the example shown in Figure 4a–d, only the red/green grating generated a response that could be confirmed as chromatic. The LFP response was stronger to blue/yellow (0.16 mV) than red/green gratings (0.14 mV), however, only the response to red/green passed the phase test. The response to luminance gratings (0.12 mV) passed our criterion of SNR (≥ 2) but not of tuning fit ($r^2 \geq 0.6$). Therefore, we only compared the red/green and blue/yellow spatial frequency tuning. Consistent with previous examples, the tuning for blue/yellow had higher spatial frequency peak (1.00 cpd), cutoff (1.65 cpd), and band-pass ratio (1.65) than the tuning for red/green (peak: 0.79 cpd; cutoff: 1.29 cpd; ratio: 1.33).

A clearer example of an LFP unresponsive to color is illustrated in Figure 4e–h. These LFPs were recorded at 15.31° eccentricity (azimuth: 15.29°, elevation: 0.71°) and responded much stronger to luminance gratings (0.46 mV) than chromatic gratings (blue/yellow: 0.27 mV, red/green: 0.28 mV). The responses to chromatic gratings did not pass our criterion of SNR (≥ 2); therefore, we only measured the tuning parameters for luminance gratings. The luminance spatial frequency tuning had a peak of 3.64 cpd, a cutoff of 5.92 cpd, and a band-pass ratio of 1.75.

To investigate the main differences between the spatial frequency tuning of LFPs to luminance and chromatic stimuli, we selected all LFP recording sites that had chromatic responses to both red/green and blue/yellow gratings, as identified by the contrast test, the phase test, or both. Then, we selected all LFP recordings that passed our criterion of SNR (≥ 2) and goodness of fit ($r^2 \geq 0.6$) for the 3 color axes, luminance, blue/yellow, and red/green. This selection resulted in 13 LFP recordings with a mean eccentricity of 8.37° (median: 8.73°). The analysis of these LFP recordings demonstrates that the peak of the spatial frequency tuning is ~3.5 times higher for luminance than chromatic gratings and ~2 times higher for blue/yellow than red/green gratings (Fig. 5a). Similarly, the spatial frequency cutoff is ~2.5 times higher for luminance than chromatic gratings (Fig. 5b). The average spatial frequency tuning was band-pass for luminance and blue/yellow gratings and low-pass for red/green gratings

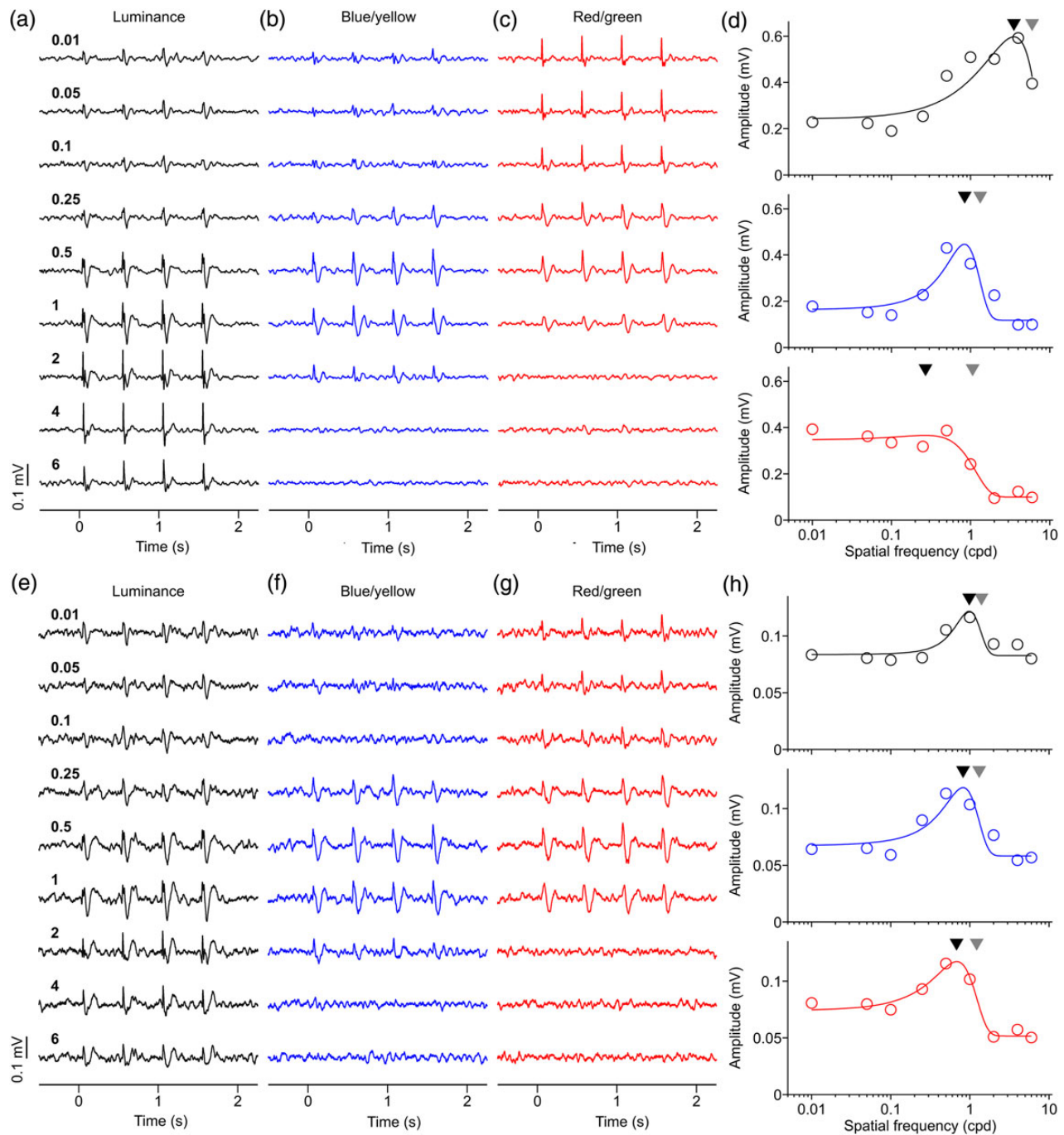


Figure 3. Two examples of LFP spatial frequency tuning. (a–d) LFP recordings with low-pass spatial frequency tuning for red/green and band-pass tuning for luminance and blue/yellow gratings. (e–h) LFP recording with band-pass spatial frequency tuning for the 3 cardinal axes of color space. Numbers on left side are spatial frequency in cycles per degree (cpd). (d) LFP spatial frequency tunings for first example. Black triangles: spatial frequency peaks. Gray triangles: spatial frequency cutoffs. Visual eccentricity: 10.43° (azimuth: 9.71°, elevation: 3.82°). (h) LFP spatial frequency tunings for second example. Visual eccentricity at 11.20° (azimuth: 10.29°, elevation: 4.41°). For both examples, LFP responses to both blue/yellow and red/green gratings were confirmed as chromatic with both contrast and phase tests. For both examples, maximum axis contrast was 94% for luminance, for blue/yellow and red/green.

(Fig. 5c). Moreover, although luminance gratings generated slightly stronger responses than chromatic gratings, (Fig. 5d, 0.34 vs. 0.27 and 0.26 mV), there was no significant difference between the average response amplitudes to blue/yellow and red/green gratings (0.27 vs. 0.26 mV, $P = 0.37$, t -test). If we classify the spatial frequency tuning of LFPs in low-pass (band-pass ratio < 1.15) and band-pass (band-pass ratio ≥ 1.15), most LFP recording sites were

either band-pass for all color axes (7/13) or band-pass for luminance and blue/yellow only (4/13). No LFP recording was band-pass for luminance and low pass for blue/yellow, or low pass for luminance and bandpass for red/green. These results demonstrate that LFPs can respond robustly to pure chromatic contrast, they can distinguish cortical sites responding to color from others responding to pure luminance, have excellent spatial

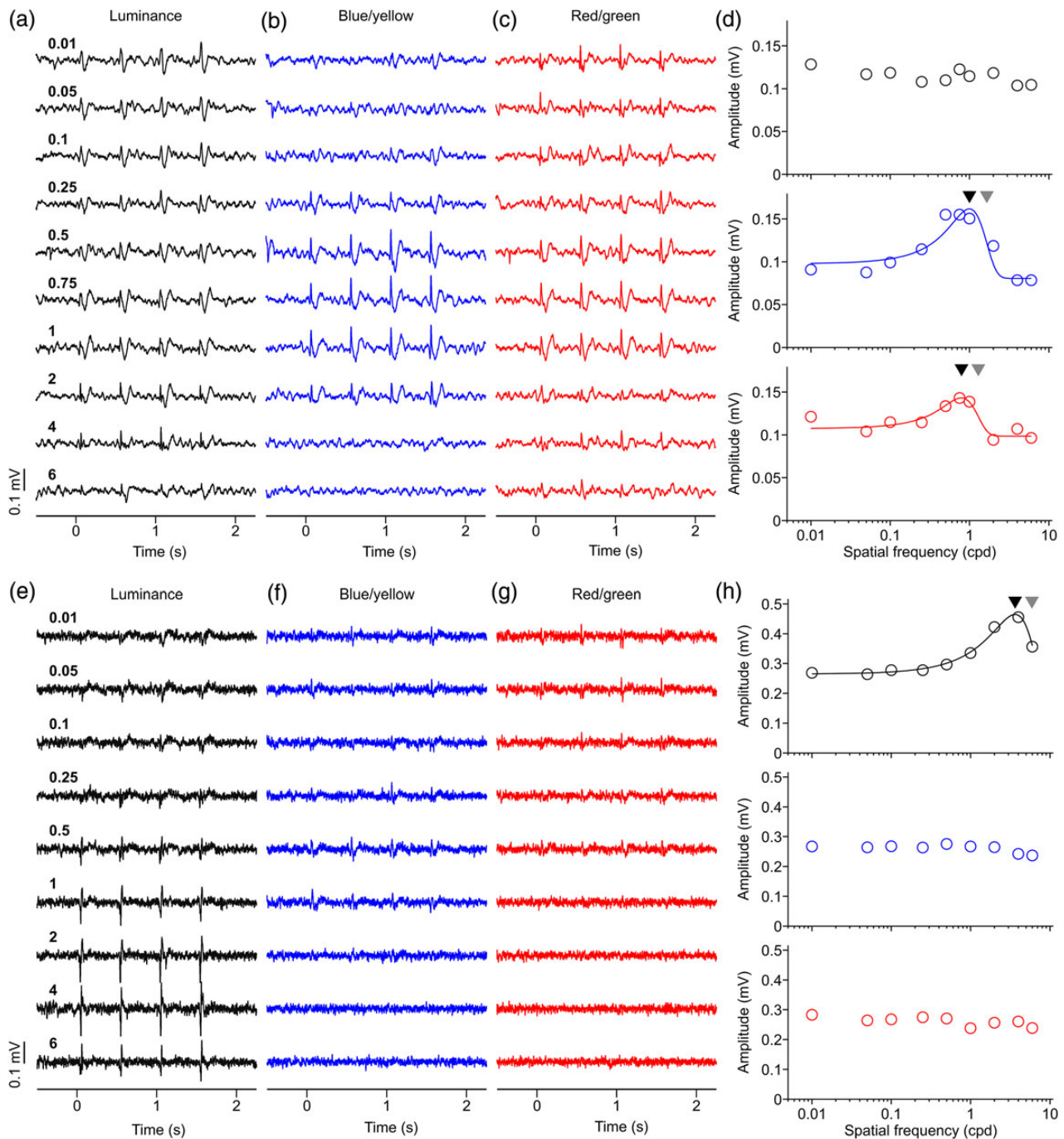


Figure 4. Two more examples of LFP spatial frequency tuning. (a–d) LFP recording with band-pass spatial frequency tuning for red/green and blue/yellow gratings. The tuning for luminance grating could not be fitted because we did not use gratings with spatial frequency high enough to reach the cutoff value. LFP chromatic response could be confirmed with the phase test for red/green gratings but not blue/yellow gratings. Maximum axis contrast was 30% for luminance and 94% for blue/yellow and red/green. Black triangles: spatial frequency peaks. Gray triangles: spatial frequency cutoffs. Visual eccentricity 8.73° (azimuth: 7.76°, elevation: 4°). (e–h) LFP recordings with band-pass spatial frequency tuning for the luminance axis, and no spatial frequency tuning for the chromatic axes. LFP responses to blue/yellow and red/green could not be confirmed as chromatic with either contrast or phase tests. Maximum axis contrast was 94% for luminance, for blue/yellow and red/green. Visual eccentricity 15.31° eccentricity (azimuth: 15.29°, elevation: 0.71°).

resolution (~5 cpd for achromatic gratings, ~2 cpd for chromatic gratings) and show stronger suppression to low spatial frequencies (band-pass tuning) for achromatic and blue/yellow gratings than red/green gratings.

Our results also demonstrate that the LFP spatial frequency peak is strongly correlated with the spatial frequency cutoff at

the 3 color axes (Fig. 5e). However, the slope of the regression was higher (and closer to 1) for luminance than chromatic gratings, indicating a more rapid decline of responses to high spatial frequencies for luminance gratings. The intercept is also more negative for luminance gratings because the cutoffs are also higher. The spatial frequency cutoff is also correlated with the

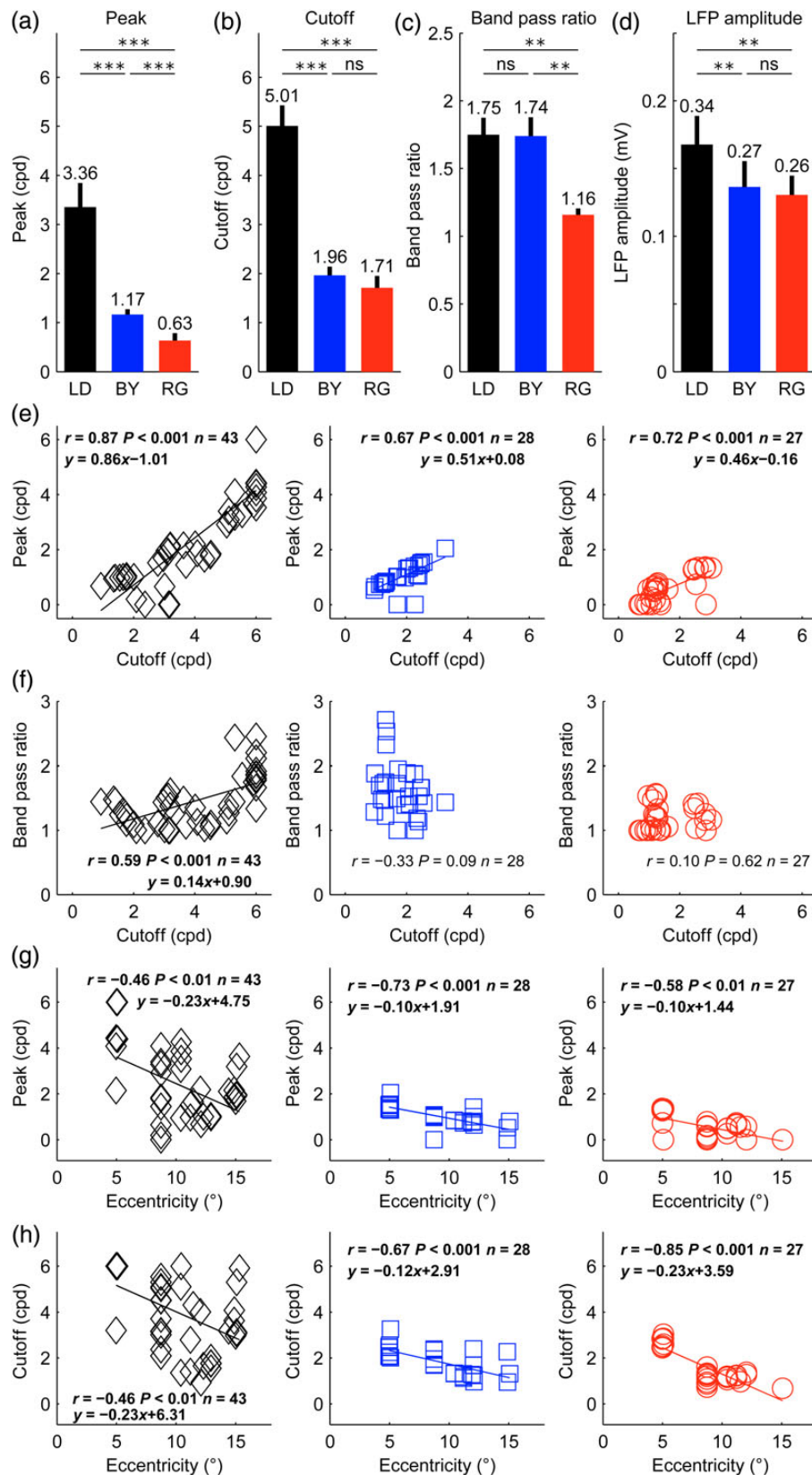


Figure 5. Spatial frequency averages and correlations for each cardinal axis. (a–d) Average differences in spatial frequency tuning for luminance (LD), blue/yellow (BY), and red/green (RG) gratings for spatial frequency peak (a), cutoff (b), band-pass ratio (c), and LFP amplitude (d). Paired t-test (***) $P < 0.001$, ** $P < 0.01$, ns = not significant). For this analysis, we used only LFP recordings ($n = 13$) with chromatic responses confirmed for both red/green and blue/yellow axes and significant spatial frequency tuning for all 3 axes ($SNR \geq 2$, $r^2 \geq 0.6$). Error bars are standard errors. (e) LFP spatial frequency cutoff is correlated with spatial frequency peak for luminance (black diamonds), blue/yellow (blue squares), and red/green gratings (red circles). (f) The LFP spatial frequency cutoff was also correlated with the band-pass ratio for luminance gratings. (g,h) Visual eccentricity is correlated with spatial frequency peak (g) and cutoff (h).

band-pass ratio measured with luminance gratings (Fig. 5f, $r = 0.59$, $P < 0.001$) but not with blue/yellow ($r = -0.33$, $P = 0.09$) or red/green gratings ($r = 0.10$, $P = 0.62$). This correlation reveals a trend for the luminance (but not chromatic) tuning to become more band-pass as the spatial frequency peak increases, a trend that may be due, at least in part, to the more restricted range of cutoffs for chromatic than luminance spatial frequency tunings (chromatic < 4 cpd; luminance ≤ 6 cpd). Both the spatial frequency peak (Fig. 5g) and cutoff (Fig. 5h) were correlated with the eccentricity of the recordings. These correlations were significant for luminance (peak: $r = -0.46$, $P < 0.01$; cutoff: $r = -0.46$, $P < 0.01$), blue/yellow (peak: $r = -0.73$, $P < 0.001$; cutoff: $r = -0.67$, $P < 0.001$), and red/green gratings (peak: $r = -0.58$, $P < 0.01$; cutoff: $r = -0.85$, $P < 0.001$). However, the slope of the regression was ~ 2 times more negative for luminance than chromatic gratings (Fig. 5g), which indicates that the LFP responses to high spatial frequencies decline more rapidly with eccentricity for luminance than chromatic gratings. These results demonstrate that the spatial resolution of LFPs decays with visual eccentricity for both chromatic and achromatic gratings and that the LFP responses showing the highest spatial resolution for luminance gratings also show the strongest suppression to low spatial frequency gratings (i.e., have higher values of band-pass ratio).

Size Tuning

To study in more detail the differences between the LFP spatial resolution to luminance and chromatic gratings, we measured the LFP size tuning in 63 recording sites. In the recording illustrated in Figure 6a–d, the maximum and half-maximum LFP response was generated by smaller luminance than chromatic gratings (maximum/half-maximum for luminance: $2.80^\circ/0.67^\circ$; blue/yellow: $6.75^\circ/2.20^\circ$, red/green: $8.01^\circ/3.75^\circ$). Moreover, large luminance gratings suppressed the LFP response ~ 2 times more strongly (0.53) than large chromatic gratings (blue/yellow: 0.27; red/green: 0.22). However, not all LFP responses were suppressed by large stimuli. In the example from Figure 6e–h, the LFP response steadily increased with stimulus size and did not saturate within the range of stimulus sizes tested (up to 12°). The LFP response in this recording was remarkably strong for luminance (0.43 mV), blue/yellow (0.38 mV), and red/green gratings (0.42 mV) and, as in the previous example, a small stimulus of 0.5° diameter generated a visible response to luminance gratings (SNR = 1.54) but not chromatic gratings (SNR = 1.21 for blue/yellow and 1.29 for red/green). On average, the maximum and half-maximum LFP responses were generated by smaller luminance gratings (maximum/half-maximum: $5.91^\circ/2.43^\circ$) than chromatic gratings (maximum/half-maximum for blue/yellow: $8.88^\circ/3.24^\circ$; for red/green: $10.65^\circ/4.87^\circ$; Fig. 7a,b). Moreover, large luminance gratings suppressed LFP responses more strongly than large chromatic gratings (Fig. 7c) even when their average LFP response amplitudes were not significantly different (Fig. 7d, luminance: 0.21 mV, blue/yellow: 0.25 mV, red/green: 0.28 mV, $P = 0.13$ for luminance vs. red/green, $P = 0.28$ for luminance vs. blue/yellow, $P = 0.60$ for blue/yellow vs. red/green, *t*-test). The percentage of LFP recordings that generated a significant response to the smallest grating tested (SNR ≥ 2 ; no criteria for tuning fit) was also larger for luminance than chromatic gratings (luminance: 22%, 13 of 60; blue/yellow: 0%, 0 of 14; red/green: 0%, 0 of 12). Moreover, the average SNR of the LFP driven by the smallest grating was significantly higher for luminance (1.85) than either blue/yellow (1.31, $P < 0.001$, *t*-test) or red/green gratings (1.37, $P < 0.001$, *t*-test). These findings further demonstrate

that the visual spatial resolution of LFP responses is higher for luminance than chromatic gratings.

Cortical Depth of LFP Recordings

To estimate the cortical depth of the recordings, we measured the polarity of the LFP generated by a luminance grating, which is negative at the top and middle layers of the cortex and becomes positive at the deep layers (Schroeder et al. 1998; Maier et al. 2011; Li et al. 2015). The LFP polarity was not correlated with the LFP spatial frequency peak, spatial frequency cutoff, preferred stimulus size, size that generated half-maximum response, the size suppression, the eccentricity of the recordings, or the amplitude of the LFP response. However, it was significantly correlated with the band-pass ratio of the spatial frequency tuning measured with blue/yellow gratings (Fig. 7f). This correlation could indicate that the layers with most positive LFPs (deep layers of the cortex) have the most pronounced band-pass spatial frequency for blue/yellow gratings. However, since we tested 8×3 correlations with LFP polarity, there is more than 5% probability that the correlation reached significance by chance. The lack of correlation between LFP polarity and the red/green or luminance band-pass ratios could be due to the smaller sample size and/or lack of recordings with positive LFPs well fit for spatial frequency tuning (Fig. 7e–g). For example, LFPs with spatial frequency cutoffs higher than 6 cpd were poorly fit with a Gaussian function because the highest spatial frequency that we tested was 6 cpd (e.g., Fig. 4a–d).

The LFP Has Higher Spatial Resolution than MUA

To compare the spatial resolution of LFP and MUA, we selected recordings in which both MUA and LFP were robustly tuned to spatial frequency. To our surprise, we found that the spatial frequency peak and cutoff were frequently higher for LFP than MUA, which indicates that LFP signals have higher spatial resolution than MUA signals. In the example illustrated in Figure 8a–d, the spatial frequency peaks and cutoffs were consistently higher for LFP than MUA for luminance, blue/yellow and red/green gratings. Also consistent with previous findings, gratings of low spatial frequencies suppressed LFP transient responses less than MUA transient responses (Bauer et al. 1995; Gieselmann and Thiele 2008; but see Ray and Maunsell 2011 for other comparisons of LFP frequency spectrum). The weaker LFP suppression to low spatial frequencies could be demonstrated with measurements of spatial frequency tuning (Fig. 8a–d, LFP is less band-pass than MUA) and size tuning (Fig. 8e–h, large stimuli suppress MUA more than LFP). In the example illustrated in Figure 8e–h, both LFP and MUA responded well to luminance and chromatic gratings; however, MUA showed stronger size suppression. On average, LFP visual responses to luminance gratings had ~ 2 times higher spatial frequency peaks and cutoffs than MUA visual responses (Fig. 9a–d), were less suppressed by low spatial frequencies (Fig. 9e,f) and responded better to large gratings than MUA (Fig. 9g–l). These differences were most pronounced when comparing LFP and MUA recorded with the same electrode tip (Fig. 9a,c,e) but they also reached significance when comparing LFPs and MUAs recorded with different electrodes (Fig. 9b,d,f). The sample of LFPs and MUAs recorded with different electrodes included significant responses to chromatic gratings, which we used to compare the LFP and MUA spatial resolution in macaque visual cortex with the spatial resolution measured with psychophysical experiments in humans. A ratio of spatial frequency cutoffs between luminance and chromatic gratings was calculated to facilitate the comparison across visual eccentricities and

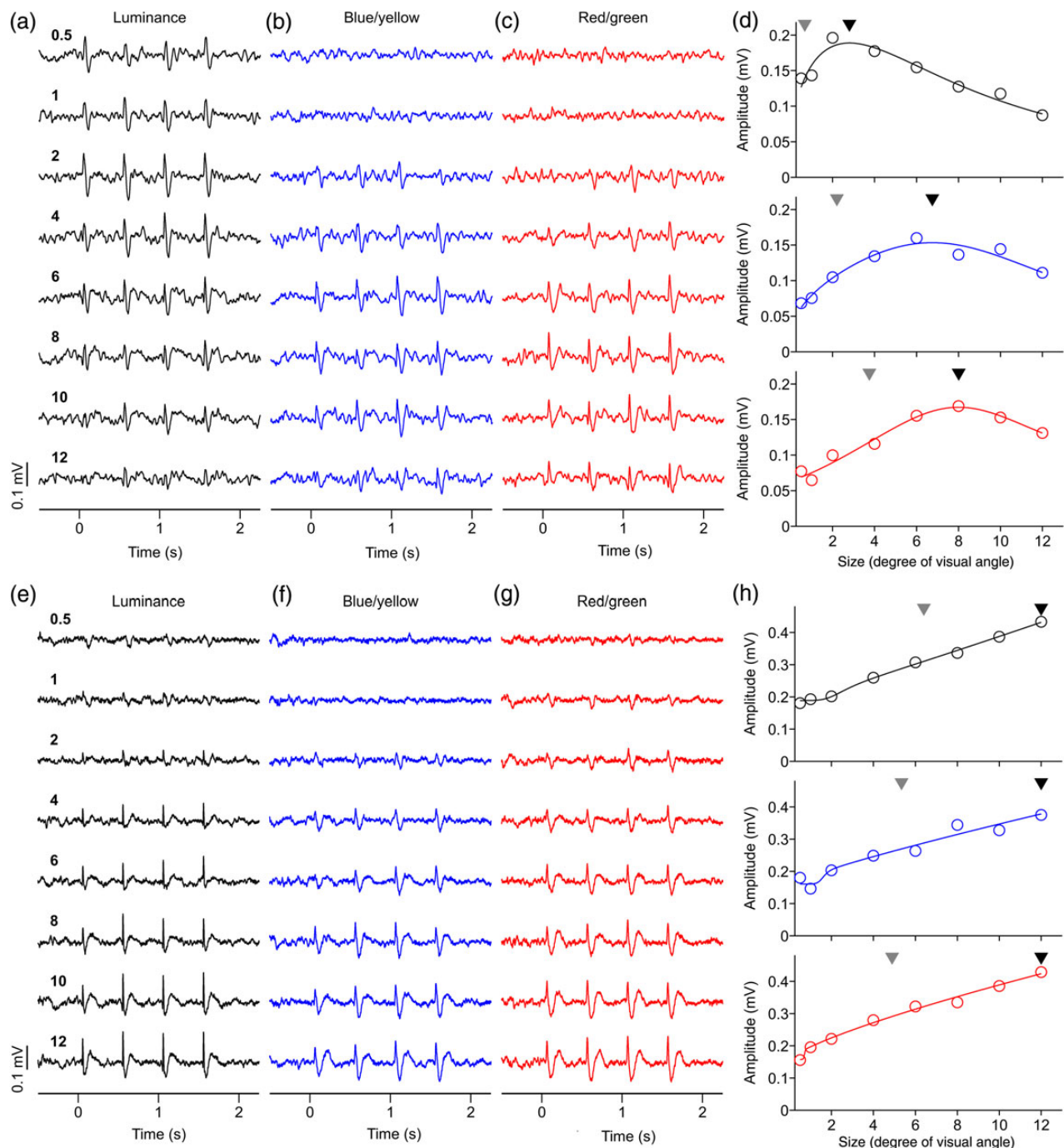


Figure 6. Examples of LFP size tuning. (a–c) LFP recordings showing pronounced response suppression to large stimuli. LFP responses to red/green gratings were confirmed as chromatic with both the contrast and phase tests. LFP responses to blue/yellow were confirmed as chromatic with the contrast test. Numbers on left side are size in degrees of visual angle. (d) LFP size tuning showing strong suppression for large sizes. Black triangle: preferred size. Gray triangle: size that generated half-maximum response. Visual eccentricity: 11.20° (azimuth: 10.29°, elevation: 4.41°). (e–g) LFP recordings showing no response suppression to large stimuli. LFP responses to red/green gratings were confirmed as chromatic with both the contrast and phase tests. LFP responses to blue/yellow were confirmed as chromatic with both the contrast and phase tests. (h) LFP size tuning showing no size suppression. Visual eccentricity: 5.09° (azimuth: 5.06°, elevation: 0.59°). For both examples, maximum axis contrast was 94% for luminance, for blue/yellow and red/green.

species (i.e., macaques and humans). The results from this analysis indicate that the chromatic/luminance ratio measured with psychophysical experiments in humans (Mullen 1985) is closer to the ratio measured with LFP than MUA activity (Fig. 10a) and that the suppression caused by luminance gratings with low spatial frequencies is much more pronounced in human vision than in both LFP and MUA recordings (Fig. 10b).

Discussion

We demonstrate that LFPs respond robustly to pure chromatic contrast through the depth of the visual cortex and that the LFP visual spatial resolution (spatial frequency cutoff) is ~2.5 times lower for chromatic gratings than luminance gratings, a value that approaches the ratio of achromatic/chromatic spatial

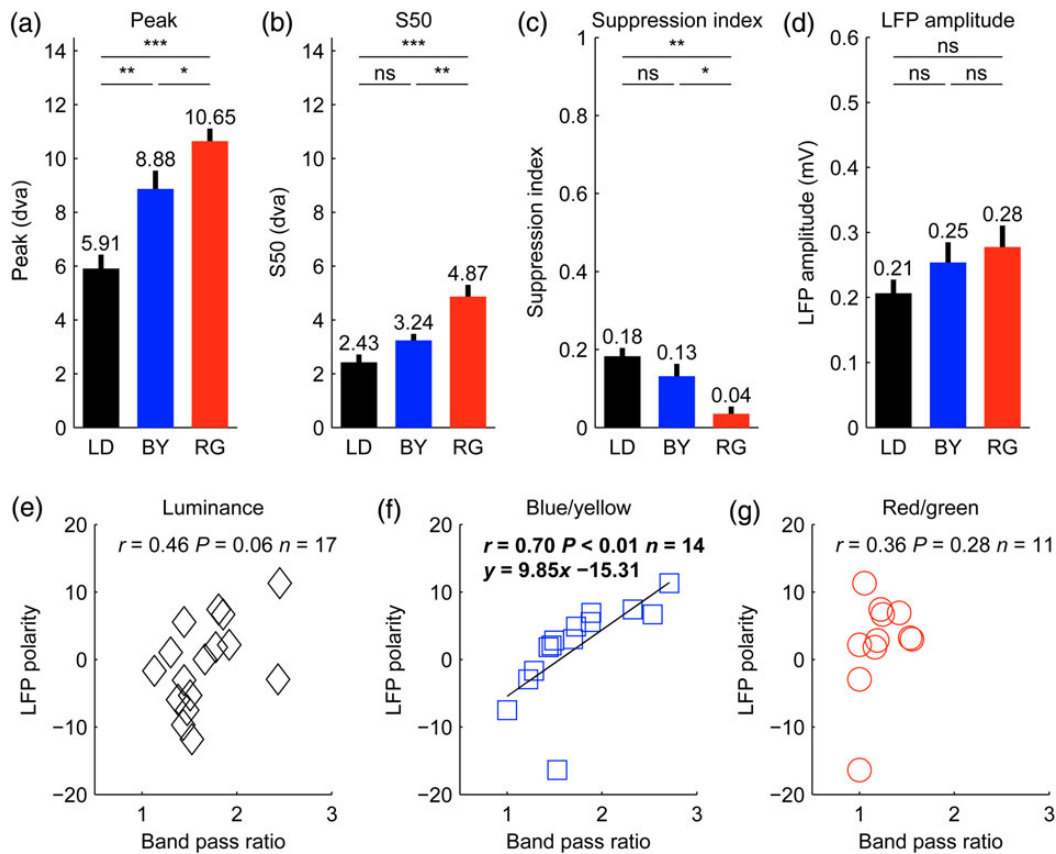


Figure 7. Size tuning and correlations for each cardinal axis (a–d). (a–d) Average differences in size tuning for luminance (LD), blue/yellow (BY), and red/green (RG) gratings for size peak (a), half-maximum response (S50, b), suppression index (c), and LFP amplitude (d). t-Test (***) $P < 0.001$, ** $P < 0.01$, * $P < 0.05$, ns = not significant). For this analysis, we selected LFP recordings that passed the color test (contrast and/or phase) for blue/yellow and/or red/green. The selected LFP recordings also had $\text{SNR} \geq 2$ and $r^2 \geq 0.6$ goodness of fit for the size tuning. The sample includes 50 LFPs measured with luminance (LD) gratings, 14 LFPs measured with blue/yellow (BY) gratings and 12 measured with red/green (RG) gratings. Error bars are standard errors. (e–g) LFP polarity was correlated with the band-pass spatial frequency ratio of blue/yellow gratings (blue squares, f) but not luminance gratings (black diamonds, e), or red/green gratings (red circles, g). However, this correlation should be interpreted with caution because we tested 8×3 correlations with LFP polarity and, therefore, there is more than 5% probability that this correlation reached significance by chance. The grating size used to measure LFP polarity was 1° . LFPs included in this analysis had to pass our criterion for signal-to-noise ratio in the responses to 1° gratings ($\text{SNR} \geq 2$). In addition, they had to pass our goodness-of-fit criterion for the spatial frequency tuning ($r^2 \geq 0.6$), which was needed to measure the spatial frequency band-pass ratio. dva: degrees of visual angle.

resolution measured with psychophysical experiments in humans (~ 3). We also show that the spatial resolution is higher for LFP than MUA cortical responses, a finding that may have implications for measurements of cortical spatial resolution with future neuronal prosthesis. Our results also demonstrate that light/dark and blue/yellow gratings suppress LFP responses more than red/green gratings and that, consistently with previous studies (Bauer et al. 1995; Gieselmann and Thiele 2008), the response suppression to low spatial frequencies is weaker for LFP than MUA. Finally, although L and M cones are 10–20 times more abundant than S cones in the macaque retina (Wikler and Rakic 1990; Martin and Grunert 1999; Roorda et al. 2001), our results suggest that the LFP visual spatial resolution in area V1 is 1.9 times higher for blue/yellow than red/green gratings.

Cortical Spread of LFP

The LFP is becoming a common measurement of neuronal population activity in multiple cortical areas including V1 (Victor et al. 1994; Kayser and Konig 2004; Jia et al. 2011; Lashgari et al. 2012), V4 (Sundberg et al. 2012; Mineault et al. 2013), MT (Liu and Newsome 2006; Khayat et al. 2010), and IT (Pesaran et al. 2002; Banerjee et al. 2010; Hagan et al. 2012). Although recordings

from spikes measure directly the neuronal output, single neuronal recordings usually last a few hours and only rarely extend for much longer (Swadlow 1985). In contrast, LFP recordings can readily remain stable for many months, which is an important advantage for the development of neuronal prosthesis (Andersen et al. 2004). LFP signals may be better related to fMRI activity (Logothetis et al. 2001) and, unlike spikes, they include subthreshold modulations in membrane potential (Mitzdorf 1985; Kamondi et al. 1998). A problem with LFPs is that their response includes multiple neurons whose number, type, geometrical arrangement and specific contributions are unknown (Einevoll et al. 2007; Linden et al. 2010, 2011; Gratiy et al. 2011; Buzsaki et al. 2012). If the neurons contributing to LFP were scattered over large brain regions, the LFPs would provide a poor measure of local neuronal activity. Fortunately, recent studies suggest that some LFP frequency bands originate from cortical regions restricted to just a few hundred microns (Swadlow and Gusev 2000; Pettersen et al. 2006; Jin et al. 2008; Katzner et al. 2009; Xing et al. 2009; Lashgari et al. 2012). While multiunit activity is thought to include neurons within $\sim 100 \mu\text{m}$ radius (Henze et al. 2000; Buzsaki 2004), the radius is $\sim 250 \mu\text{m}$ for LFP (Katzner et al. 2009; Xing et al. 2009; Lashgari et al. 2012) and 2–5 mm for gradient echo BOLD fMRI signals (Ugurbil et al. 2003; Shmuel et al.

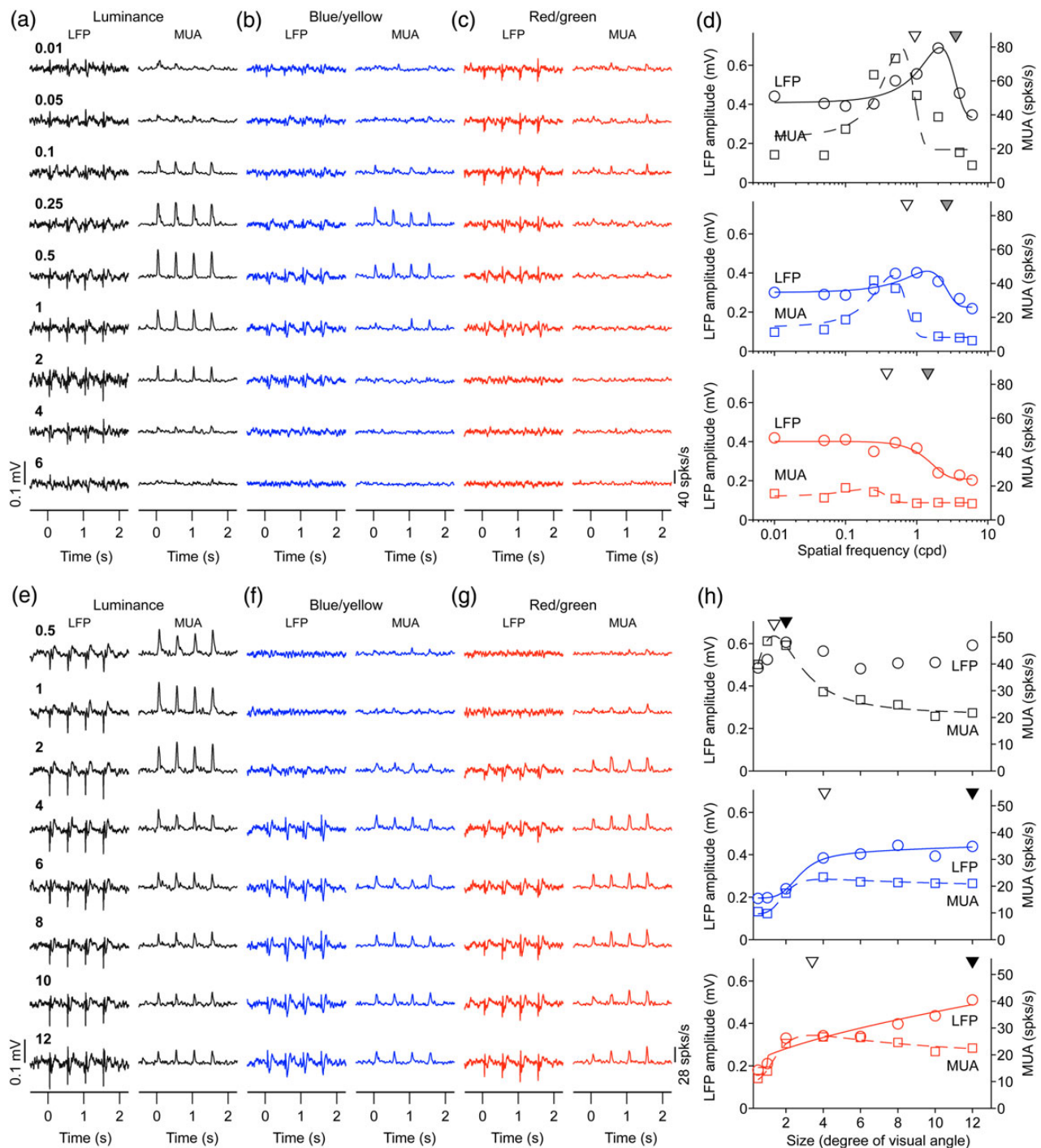


Figure 8. LFP has higher spatial resolution and is less suppressed by low spatial frequencies than MUA. (a–c) LFP and MUA responses to different spatial frequencies. (d) Spatial frequency tuning for LFP (continuous lines) and MUA (discontinuous lines). The spatial frequency peak is higher for LFP (gray triangle) than MUA (open triangle). (e–g) LFP and MUA responses to gratings of different sizes. (h) Size tuning for LFP (circles and solid lines) and MUA (squares and dashed lines). Scale is shown on the left for LFP amplitude and on the right for MUA.

2007). Therefore, the volume of neurons recorded by LFP has a radius that is at least one order of magnitude smaller than for fMRI signals.

LFP Chromatic Selectivity in Area V1

The limited $\sim 250 \mu\text{m}$ spread of LFP is consistent with studies demonstrating robust LFP stimulus selectivity for retinotopy,

eye input, orientation, direction, and even spatial phase (Liu and Newsome 2006; Berens et al. 2008; Katzner et al. 2009; Xing et al. 2009; Lashgari et al. 2012; Mineault et al. 2013). Surprisingly, LFP selectivity for equiluminant chromatic stimuli has only been studied in one previous article (Victor et al. 1994), perhaps because LFP chromatic responses were thought to be weak. Weak chromatic responses would be expected if the spatial resolution of the LFP was too low to measure in cortical cells restricted to

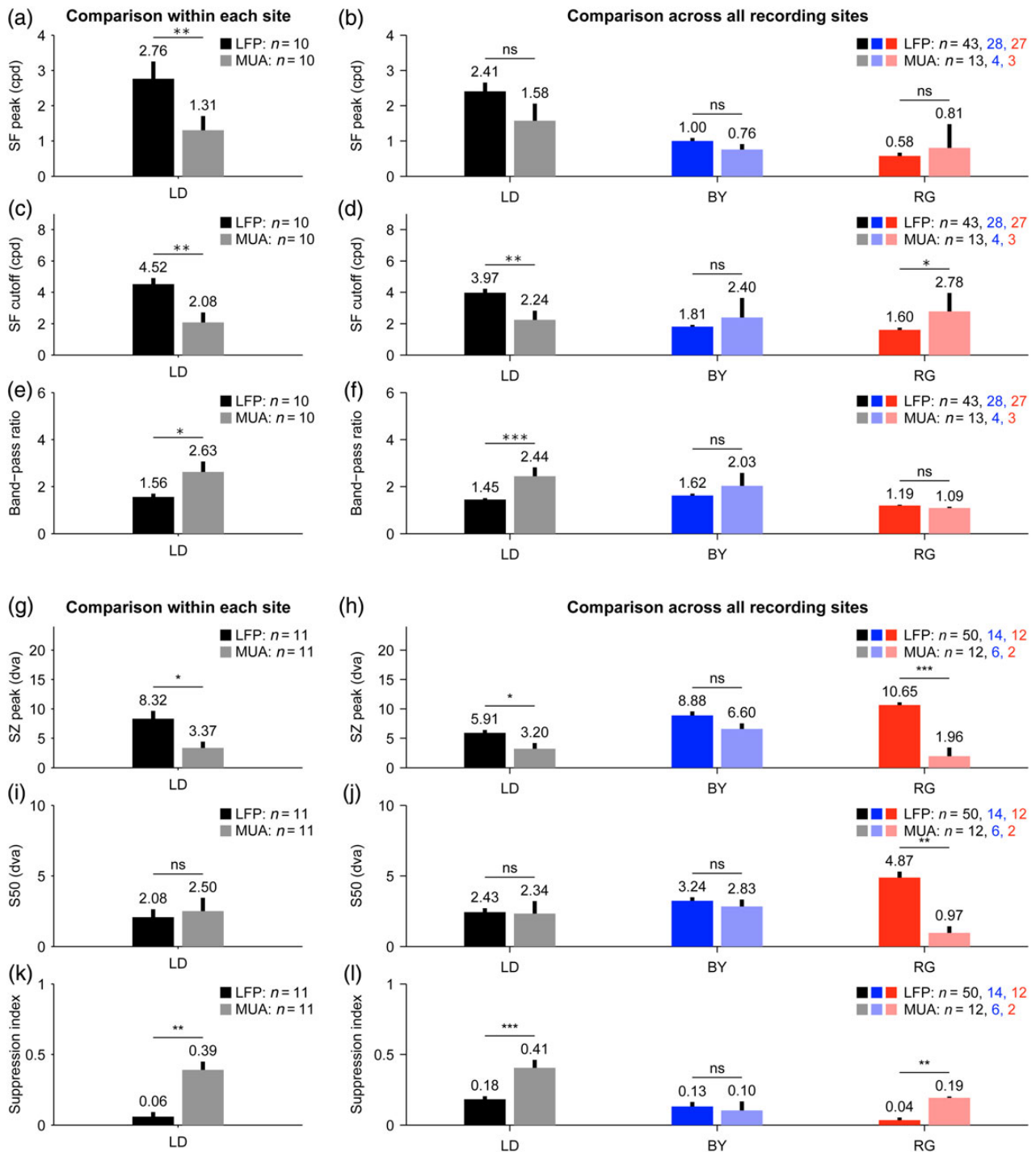


Figure 9. LFP is less suppressed by large stimuli than MUA. (a–l) Average values of LFP (dark colors) and MUA (light colors) of spatial frequency peak (a,b), cutoff (c,d), band-pass ratio (e,f), size peak (g,h), S50 (i,j), and suppression index (k,l). Left panels (a,c,e,g,i,k) show LFP/MUA recordings from the same electrode tip. Right panels (b,d,f,h,j,l) show LFP/MUA recordings from the same or different electrode tips. The number of recording sites is shown at the upper right corner of each plot. t-Test (** $P < 0.001$, ** $P < 0.01$, * $P < 0.05$, ns = not significant). dva: degrees of visual angle.

thin layers [thickness of layer 4C_{beta} ~170 μm (O’Kusky and Colonnier 1982; Hawken et al. 1988)] or small blobs [diameter of blobs ~150–200 μm , (Horton and Hubel 1981; Horton 1984; Livingstone and Hubel 1984)] and if the cells generating chromatic responses were few in number, as some studies suggest (~10% according to Conway and Livingstone (2006)). However, recent

studies indicate that LFP signals can be sometimes restricted to ~200 μm within cortical layer 4 (Swadlow and Gusev 2000; Swadlow 2002; Jin et al. 2008; Stoelzel et al. 2008) and that ~40% of V1 neurons respond to equiluminant chromatic gratings [75% of these also respond to luminance (Johnson et al. 2001)]. Consistently with the results from Johnson et al. (2001), 41% of

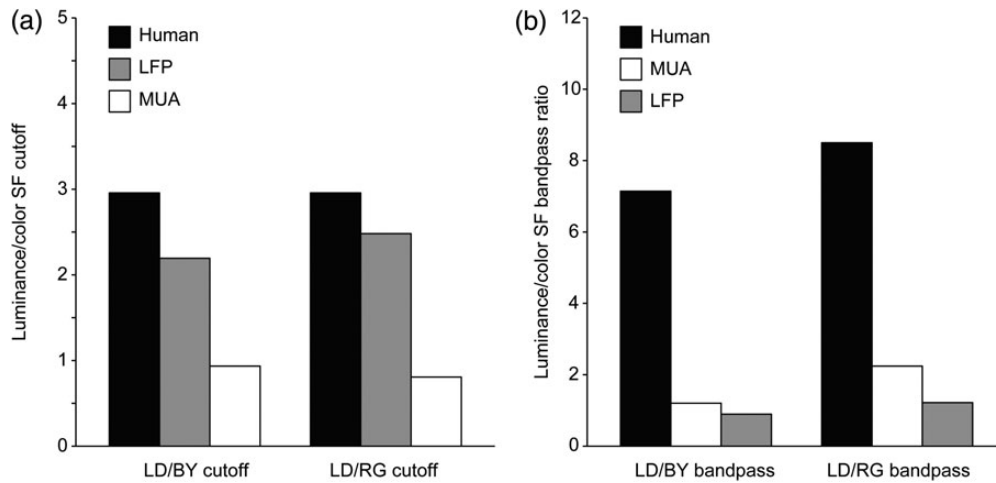


Figure 10. Comparison of achromatic/chromatic spatial resolution and band-pass ratio among LFP, MUA, and human psychophysics. (a) The ratio of luminance/color spatial frequency cutoff measured with human psychophysics was closer to the ratio measured with LFP than MUA in macaques, both for blue/yellow (BY) and red/green (RG) gratings. (b) The ratio of luminance/color bandpass measured with human psychophysics was much higher than that measured with LFP and MUA in macaques. Values for human psychophysics were obtained from Mullen (1985). LD, light/dark gratings.

our LFP recordings responded to equiluminant red/green gratings (27/66) and 42% to blue/yellow gratings (28/66). Also consistently with Conway and Livingstone (2006), who found few cortical neurons responding to small color patches, many of our LFPs responded to small luminance gratings but only 5% responded to small red/green gratings (40 vs. 2, for 2° grating size).

Previous studies claimed that color-opponent cells were concentrated in blobs within the superficial layers of the cortex (Livingstone and Hubel 1984; Ts'o and Gilbert 1988; Landisman and Ts'o 2002b); however, other studies failed to confirm these findings (Lennie et al. 1990; Leventhal et al. 1995). Because cortical blobs are strongly driven by equiluminant chromatic stimuli with low spatial frequency (Tootell et al. 1988; Lu and Roe 2007; Xiao et al. 2007; Valverde Salzmán et al. 2012), it has been suggested that it is the low spatial frequency and not the color opponency that is clustered (Silverman et al. 1989). Color-opponent cells may also cluster in other cortical compartments and/or layers (Dow and Vautin 1987; Lund 1988; Chatterjee and Callaway 2003); however, the segregation of color in visual cortex remains a matter of debate. Our results are consistent with the notion that neurons responsive to chromatic contrast cluster in visual cortex (Livingstone and Hubel 1988; Landisman and Ts'o 2002a; Xiao et al. 2007). If the 40% of neurons responding to equiluminant red/green gratings (Johnson et al. 2001, 2004) were widely distributed in area V1, we would expect LFP responses to be ~2 times stronger to luminance than chromatic gratings [40% of V1 cells respond to color; 90% of V1 cells respond to luminance, according to Johnson et al. (2001, 2004)]. However, the average amplitude of the LFP responses was comparable for luminance and chromatic gratings, when measured with optimal grating sizes. Also, our finding that some LFP recording sites responded only to luminance gratings demonstrates that neurons responsive to chromatic gratings are not homogeneously distributed in area V1.

Technical Limitations in the Measurements of Chromatic Responses in Visual Cortex

A V1 cell driven by equiluminant chromatic contrast may not necessarily be involved in color encoding and may not even receive input from the parvocellular pathway. For example a small mismatch in the strength of the cone inputs to a magnocellular

retinal ganglion cell could make the cell responsive to chromatic contrast. However, such a magnocellular cell would behave more as a miscalibrated luminance photometer than a color detector (Gegenfurtner et al. 1994). Luminance artifacts may arise from a variety of sources when using equiluminant stimuli, including chromatic aberrations, unbalanced L and M cone inputs (Shapley 1990), and variations in macular pigment density across the retina (Snodderly, Auran, et al. 1984; Cottaris 2003). Chromatic aberrations can also cause luminance artifacts in humans when equiluminant gratings are presented at high spatial frequencies (>8 cpd) (Sekiguchi et al. 1993). A V1 cell will be most useful to encode color if it responds to an equiluminant chromatic grating more strongly than to a luminance grating with the same cone contrast. In this study, we identified LFP chromatic responses based on this contrast principle and a phase test inspired by previous measurements in single neurons and fMRI (Gegenfurtner et al. 1994; Goddard et al. 2010).

Differences in LFP Responses to Chromatic and Luminance Gratings

Our results demonstrate that the spatial resolution of LFPs is higher (and the tuning more band-pass) for luminance than chromatic red/green gratings. These results are consistent with a previous LFP study in area V1 (Victor et al. 1994) and with measurements of human contrast sensitivity (Mullen 1985). Surprisingly, our results also demonstrate that the spatial frequency peak is higher for blue/yellow than red/green gratings even if L and M cones are more abundant than S cones in the macaque retina (Wikler and Rakic 1990; Martin and Grunert 1999; Roorda et al. 2001). Previous measurements of spatial frequency tuning in the LGN of monkeys demonstrated that some koniocellular cells have spatial frequency peaks and cutoffs that are intermediate between parvocellular and magnocellular cells (Norton et al. 1988; Weltzien et al. 2014). Therefore, taken together, these results indicate that visual spatial resolution of cortical responses for blue/yellow gratings is better than expected from the density of the S cone array in the retina.

Our results also indicate that the LFP response suppression driven by low spatial frequencies can be 4.5 times stronger for luminance than chromatic red/green gratings (Fig. 7c), a ratio that is

~2 times greater than what has been reported for cortical single neurons recorded under anesthesia (Solomon et al. 2004). At the same time, we found that the response suppression to low spatial frequencies was weaker in LFP than MUA (see also Bauer et al. 1995; Gieselmann and Thiele 2008). Taken together, these results suggest that LFPs respond better than MUA to luminance gratings with low spatial frequency and that LFPs differentiate better the low spatial frequencies from achromatic and chromatic gratings than single neurons.

We have also shown that low spatial frequencies suppress most strongly the LFPs that have the highest spatial frequency cutoffs. Because the spatial frequency cutoff is highest at the fovea, low spatial frequencies should suppress LFPs mostly at the center of vision. This low spatial frequency suppression could serve to restrict foveal cortical responses to the finest details and highest spatial frequencies of the image. Consistent with this interpretation, low spatial frequency suppression was much stronger for luminance than chromatic gratings as the spatial resolution was also higher for luminance gratings. Interestingly, the decay of LFP responses to high spatial frequencies was also steeper for luminance than chromatic gratings, which could indicate that luminance gratings suppress LFP responses more than chromatic gratings both at low and high spatial frequencies.

Finally, it was surprising to find that the cortical spatial resolution for luminance and chromatic gratings was higher when measured with LFP than spiking activity. A possible explanation for this result is that gratings with high spatial frequency are able to suppress spiking activity but not the subthreshold responses contained in the LFP signals. An alternative explanation is that LFPs pool from a larger population of cells than MUA and are more likely to include cells with higher spatial frequency cutoffs. Differences in the neuronal pool size could also explain why human achromatic/chromatic spatial resolution is closer to the LFP than MUA achromatic/chromatic ratio (i.e., the LFP neuronal pool may be closer in size to the critical population needed to perceive a high spatial frequency grating). The reason why humans and monkeys have better spatial resolution for achromatic than chromatic gratings is unclear but could reflect the lower number of cortical cells responding to color versus luminance.

In conclusion, LFP recordings provide an excellent approach to measure population responses from cortical neurons to chromatic and achromatic stimuli. They respond robustly to both luminance and color patterns, they have better spatial resolution and weaker low spatial frequency suppression than spiking activity and they provide a better estimate of the spatial resolution ratio for achromatic/chromatic gratings measured with psychophysical experiments in humans. Because LFP recordings are also more stable than spiking activity, LFPs seem an excellent signal to guide the implant of visual cortical prosthesis and monitor the response properties of the neuronal populations that are being stimulated.

Funding

We are grateful to the National Institute of Health (grant numbers EY02067901, EY07556, and EY13312) for funding support, and for a DFG Research Fellowship (KR 4062/1-1) to J.K. Funding to pay the Open Access publication charges for this article was provided by the National Institute of Health grant number EY020679.

Notes

Conflict of Interest: None declared.

References

- Andersen RA, Musallam S, Pesaran B. 2004. Selecting the signals for a brain-machine interface. *Curr Opin Neurobiol.* 14:720–726.
- Banerjee A, Dean HL, Pesaran B. 2010. A likelihood method for computing selection times in spiking and local field potential activity. *J Neurophysiol.* 104:3705–3720.
- Bauer R, Brosch M, Eckhorn R. 1995. Different rules of spatial summation from beyond the receptive field for spike rates and oscillation amplitudes in cat visual cortex. *Brain Res.* 669:291–297.
- Berens P, Keliris GA, Ecker AS, Logothetis NK, Tolias AS. 2008. Comparing the feature selectivity of the gamma-band of the local field potential and the underlying spiking activity in primate visual cortex. *Front Syst Neurosci.* 2:2.
- Buzsaki G. 2004. Large-scale recording of neuronal ensembles. *Nat Neurosci.* 7:446–451.
- Buzsaki G, Anastassiou CA, Koch C. 2012. The origin of extracellular fields and currents—EEG, ECoG, LFP and spikes. *Nat Rev Neurosci.* 13:407–420.
- Chatterjee S, Callaway E. 2003. Parallel colour-opponent pathways to primary visual cortex. *Nature.* 426:668–671.
- Chen Y, Martinez-Conde S, Macknik SL, Bereshpolova Y, Swadlow HA, Alonso J-M. 2008. Task difficulty modulates the activity of specific neuronal populations in primary visual cortex. *Nat Neurosci.* 11:974–982.
- Conway BR, Livingstone MS. 2006. Spatial and temporal properties of cone signals in alert macaque primary visual cortex. *J Neurosci.* 26:10826–10846.
- Cottaris NP. 2003. Artifacts in spatiochromatic stimuli due to variations in preretinal absorption and axial chromatic aberration: implications for color physiology. *J Opt Soc Am A Opt Image Sci Vis.* 20:1694–1713.
- Derrington AM, Krauskopf J, Lennie P. 1984. Chromatic mechanisms in lateral geniculate nucleus of macaque. *J Physiol.* 357:241–265.
- Derrington AM, Lennie P. 1984. Spatial and temporal contrast sensitivities of neurons in lateral geniculate nucleus of macaque. *J Physiol.* 357:219–240.
- Dow BM, Vautin RG. 1987. Horizontal segregation of color information in the middle layers of foveal striate cortex. *J Neurophysiol.* 57:712–739.
- Einevoll GT, Petterson KH, Devor A, Ulbert I, Halgren E, Dale AM. 2007. Laminar population analysis: estimating firing rates and evoked synaptic activity from multielectrode recordings in rat barrel cortex. *J Neurophysiol.* 97:2174–2190.
- Gegenfurtner KR, Kiper DC, Beusmans JM, Carandini M, Zaidi Q, Movshon JA. 1994. Chromatic properties of neurons in macaque MT. *Vis Neurosci.* 11:455–466.
- Gieselmann MA, Thiele A. 2008. Comparison of spatial integration and surround suppression characteristics in spiking activity and the local field potential in macaque V1. *Eur J Neurosci.* 28:447–459.
- Goddard E, Mannion DJ, McDonald JS, Solomon SG, Clifford CWG. 2010. Combination of subcortical color channels in human visual cortex. *J Vis.* 10:25.
- Gratny SL, Devor A, Einevoll GT, Dale AM. 2011. On the estimation of population-specific synaptic currents from laminar multielectrode recordings. *Front Neuroinform.* 5:32.
- Hagan MA, Dean HL, Pesaran B. 2012. Spike-field activity in parietal area LIP during coordinated reach and saccade movements. *J Neurophysiol.* 107:1275–1290.
- Hawken MJ, Parker AJ, Lund JS. 1988. Laminar organization and contrast sensitivity of direction-selective cells in the striate cortex of the Old World monkey. *J Neurosci.* 8:3541–3548.

- Henze DA, Borhegyi Z, Csicsvari J, Mamiya A, Harris KD, Buzsaki G. 2000. Intracellular features predicted by extracellular recordings in the hippocampus in vivo. *J Neurophysiol.* 84:390–400.
- Hicks TP, Lee BB, Vidyasagar TR. 1983. The responses of cells in macaque lateral geniculate nucleus to sinusoidal gratings. *J Physiol.* 337:183–200.
- Horton JC. 1984. Cytochrome oxidase patches: a new cytoarchitectonic feature of monkey visual cortex. *Philos Trans R Soc Lond B Biol Sci.* 304:199–253.
- Horton JC, Hubel DH. 1981. Regular patchy distribution of cytochrome oxidase staining in primary visual cortex of macaque monkey. *Nature.* 292:762–764.
- Jia X, Smith MA, Kohn A. 2011. Stimulus selectivity and spatial coherence of gamma components of the local field potential. *J Neurosci.* 31:9390–9403.
- Jin JZ, Weng C, Yeh CI, Gordon JA, Ruthazer ES, Stryker MP, Swadlow HA, Alonso JM. 2008. On and off domains of geniculate afferents in cat primary visual cortex. *Nat Neurosci.* 11:88–94.
- Johnson EN, Hawken MJ, Shapley R. 2004. Cone inputs in macaque primary visual cortex. *J Neurophysiol.* 91:2501–2514.
- Johnson EN, Hawken MJ, Shapley R. 2008. The orientation selectivity of color-responsive neurons in macaque V1. *J Neurosci.* 28:8096–8106.
- Johnson EN, Hawken MJ, Shapley R. 2001. The spatial transformation of color in the primary visual cortex of the macaque monkey. *Nat Neurosci.* 4:409–416.
- Kamondi A, Acsady L, Wang XJ, Buzsaki G. 1998. Theta oscillations in somata and dendrites of hippocampal pyramidal cells in vivo: activity-dependent phase-precession of action potentials. *Hippocampus.* 8:244–261.
- Katzner S, Nauhaus I, Benucci A, Bonin V, Ringach DL, Carandini M. 2009. Local origin of field potentials in visual cortex. *Neuron.* 61:35–41.
- Kayser C, Konig P. 2004. Stimulus locking and feature selectivity prevail in complementary frequency ranges of V1 local field potentials. *Eur J Neurosci.* 19:485–489.
- Khayat PS, Niebergall R, Martinez-Trujillo JC. 2010. Frequency-dependent attentional modulation of local field potential signals in macaque area MT. *J Neurosci.* 30:7037–7048.
- Landisman CE, Ts'o DY. 2002a. Color processing in macaque striate cortex: electrophysiological properties. *J Neurophysiol.* 87:3138–3151.
- Landisman CE, Ts'o DY. 2002b. Color processing in macaque striate cortex: relationships to ocular dominance, cytochrome oxidase, and orientation. *J Neurophysiol.* 87:3126–3137.
- Lashgari R, Li X, Chen Y, Kremkow J, Bereshpolova Y, Swadlow HA, Alonso JM. 2012. Response properties of local field potentials and neighboring single neurons in awake primary visual cortex. *J Neurosci.* 32:11396–11413.
- Lee BB, Kremers J, Yeh T. 1998. Receptive fields of primate retinal ganglion cells studied with a novel technique. *Vis Neurosci.* 15:161–175.
- Lennie P, Krauskopf J, Sclar G. 1990. Chromatic mechanisms in striate cortex of macaque. *J Neurosci.* 10:649–669.
- Leventhal AG, Thompson KG, Liu D, Zhou Y, Ault SJ. 1995. Concomitant sensitivity to orientation, direction, and color of cells in layers 2, 3, and 4 of monkey striate cortex. *J Neurosci.* 15:1808–1818.
- Li X, Chen Y, Lashgari R, Bereshpolova Y, Swadlow HA, Lee BB, Alonso JM. 2015. Mixing of chromatic and luminance retinal signals in primate area V1. *Cereb Cortex.* 25:1920–1937.
- Linden H, Pettersen KH, Einevoll GT. 2010. Intrinsic dendritic filtering gives low-pass power spectra of local field potentials. *J Comput Neurosci.* 29:423–444.
- Linden H, Tetzlaff T, Potjans TC, Pettersen KH, Grun S, Diesmann M, Einevoll GT. 2011. Modeling the spatial reach of the LFP. *Neuron.* 72:859–872.
- Liu J, Newsome WT. 2006. Local field potential in cortical area MT: stimulus tuning and behavioral correlations. *J Neurosci.* 26:7779–7790.
- Livingstone M, Hubel D. 1984. Anatomy and physiology of a color system in the primate visual cortex. *J Neurosci.* 4:309–356.
- Livingstone M, Hubel D. 1988. Segregation of form, color, movement, and depth: anatomy, physiology, and perception. *Science.* 240:740–749.
- Logothetis N, Pauls J, Augath M, Trinath T, Oeltermann A. 2001. Neurophysiological investigation of the basis of the fMRI signal. *Nature.* 412:150–157.
- Lu HD, Roe AW. 2007. Functional organization of color domains in V1 and V2 of macaque monkey revealed by optical imaging. *Cereb Cortex.* 18:516–533.
- Lund JS. 1988. Anatomical organization of macaque monkey striate visual cortex. *Annu Rev Neurosci.* 11:253–288.
- MacLeod D, Boynton R. 1979. Chromaticity diagram showing cone excitation by stimuli of equal luminance. *J Opt Soc Am.* 69:1183–1186.
- Maier A, Aura CJ, Leopold DA. 2011. Infragranular sources of sustained local field potential responses in macaque primary visual cortex. *J Neurosci.* 31:1971–1980.
- Martin PR, Grunert U. 1999. Analysis of the short wavelength-sensitive ('blue') cone mosaic in the primate retina: comparison of New World and Old World monkeys. *J Comp Neurol.* 406:1–14.
- Mineault PJ, Zanos TP, Pack CC. 2013. Local field potentials reflect multiple spatial scales in V4. *Front Comput Neurosci.* 7:21.
- Mitzdorf U. 1985. Current source-density method and application in cat cerebral cortex: investigation of evoked potentials and EEG phenomena. *Physiol Rev.* 65:37–100.
- Mullen KT. 1985. The contrast sensitivity of human colour vision to red-green and blue-yellow chromatic gratings. *J Physiol.* 359:381–400.
- Norton TT, Casagrande VA, Irvin GE, Sesma MA, Petry HM. 1988. Contrast-sensitivity functions of W-, X-, and Y-like relay cells in the lateral geniculate nucleus of bush baby, *Galago crassicaudatus*. *J Neurophysiol.* 59:1639–1656.
- O'Kusky J, Colonnier M. 1982. A laminar analysis of the number of neurons, glia, and synapses in the adult cortex (area 17) of adult macaque monkeys. *J Comp Neurol.* 210:278–290.
- Pesaran B, Pezaris JS, Sahani M, Mitra PP, Andersen RA. 2002. Temporal structure in neuronal activity during working memory in macaque parietal cortex. *Nat Neurosci.* 5:805–811.
- Pettersen KH, Devor A, Ulbert I, Dale AM, Einevoll GT. 2006. Current-source density estimation based on inversion of electrostatic forward solution: effects of finite extent of neuronal activity and conductivity discontinuities. *J Neurosci Methods.* 154:116–133.
- Ray S, Maunsell JH. 2011. Different origins of gamma rhythm and high-gamma activity in macaque visual cortex. *PLoS Biol.* 9:e1000610.
- Reid RC, Shapley RM. 2002. Space and time maps of cone photoreceptor signals in macaque lateral geniculate nucleus. *J Neurosci.* 22:6158–6175.
- Reid RC, Shapley RM. 1992. Spatial structure of cone inputs to receptive fields in primate lateral geniculate nucleus. *Nature.* 356:716–718.
- Ringach DL, Sapiro G, Shapley R. 1997. A subspace reverse-correlation technique for the study of visual neurons. *Vision Res.* 37:2455–2464.

- Roorda A, Metha AB, Lennie P, Williams DR. 2001. Packing arrangement of the three cone classes in primate retina. *Vision Res.* 41:1291–1306.
- Roy S, Jayakumar J, Martin PR, Dreher B, Saalman YB, Hu D, Vidyasagar TR. 2009. Segregation of short-wavelength-sensitive (S) cone signals in the macaque dorsal lateral geniculate nucleus. *Eur J Neurosci.* 30:1517–1526.
- Schroeder CE, Mehta AD, Givre SJ. 1998. A spatiotemporal profile of visual system activation revealed by current source density analysis in the awake macaque. *Cereb Cortex.* 8:575–592.
- Sekiguchi N, Williams DR, Brainard DH. 1993. Aberration-free measurements of the visibility of isoluminant gratings. *J Opt Soc Am A Opt Image Sci Vis.* 10:2105–2117.
- Shapley R. 1990. Visual sensitivity and parallel retinocortical channels. *Annu Rev Psychol.* 41:635–658.
- Shapley R, Hawken MJ. 2011. Color in the Cortex: single- and double-opponent cells. *Vision Res.* 51:701–717.
- Shmuel A, Yacoub E, Chaimow D, Logothetis NK, Ugurbil K. 2007. Spatio-temporal point-spread function of fMRI signal in human gray matter at 7 Tesla. *Neuroimage.* 35:539–552.
- Silverman MS, Groszof DH, De Valois RL, Elfar SD. 1989. Spatial-frequency organization in primate striate cortex. *Proc Natl Acad Sci USA.* 86:711–715.
- Smith VC, Pokorny J. 1975. Spectral sensitivity of the foveal cone photopigments between 400 and 500 nm. *Vision Res.* 15:161–171.
- Snodderly D, Auran J, Delori F. 1984. The macular pigment. II. Spatial distribution in primate retinas. *Invest Ophthalmol Vis Sci.* 25:674–685.
- Snodderly D, Brown P, Delori F, Auran J. 1984. The macular pigment. I. Absorbance spectra, localization, and discrimination from other yellow pigments in primate retinas. *Invest Ophthalmol Vis Sci.* 25:660–673.
- Solomon SG, Peirce JW, Lennie P. 2004. The impact of suppressive surrounds on chromatic properties of cortical neurons. *J Neurosci.* 24:148–160.
- Stoelzel CR, Bereshpolova Y, Gusev AG, Swadlow HA. 2008. The impact of an LGNd impulse on the awake visual cortex: synaptic dynamics and the sustained/transient distinction. *J Neurosci.* 28:5018–5028.
- Sun H, Smithson HE, Zaidi Q, Lee BB. 2006. Specificity of cone inputs to macaque retinal ganglion cells. *J Neurophysiol.* 95:837–849.
- Sundberg KA, Mitchell JF, Gawne TJ, Reynolds JH. 2012. Attention influences single unit and local field potential response latencies in visual cortical area V4. *J Neurosci.* 32:16040–16050.
- Swadlow HA. 1985. Physiological properties of individual cerebral axons studied in vivo for as long as one year. *J Neurophysiol.* 54:1346–1362.
- Swadlow HA. 2002. Thalamocortical control of feed-forward inhibition in awake somatosensory ‘barrel’ cortex. *Philos Trans R Soc Lond B Biol Sci.* 357:1717–1727.
- Swadlow HA, Bereshpolova Y, Bezudnaya T, Cano M, Stoelzel CR. 2005. A multi-channel, implantable microdrive system for use with sharp, ultra-fine “Reitboeck” microelectrodes. *J Neurophysiol.* 93:2959–2965.
- Swadlow HA, Gusev AG. 2000. The influence of single VB thalamocortical impulses on barrel columns of rabbit somatosensory cortex. *J Neurophysiol.* 83:2802–2813.
- Szmajda BA, Buzas P, Fitzgibbon T, Martin PR. 2006. Geniculocortical relay of blue-off signals in the primate visual system. *Proc Natl Acad Sci USA.* 103:19512–19517.
- Tailby C, Solomon SG, Lennie P. 2008. Functional asymmetries in visual pathways carrying S-cone signals in macaque. *J Neurosci.* 28:4078–4087.
- Tailby C, Szmajda BA, Buzas P, Lee BB, Martin PR. 2008. Transmission of blue (S) cone signals through the primate lateral geniculate nucleus. *J Physiol.* 586:5947–5967.
- Thorell LG, De Valois RL, Albrecht DG. 1984. Spatial mapping of monkey V1 cells with pure color and luminance stimuli. *Vision Res.* 24:751–769.
- Tootell RB, Silverman MS, Hamilton SL, De Valois RL, Switkes E. 1988. Functional anatomy of macaque striate cortex. III. Color. *J Neurosci.* 8:1569–1593.
- Ts'o DY, Gilbert CD. 1988. The organization of chromatic and spatial interactions in the primate striate cortex. *J Neurosci.* 8:1712–1727.
- Ugurbil K, Toth L, Kim DS. 2003. How accurate is magnetic resonance imaging of brain function? *Trends Neurosci.* 26:108–114.
- Valverde Salzman MF, Bartels A, Logothetis NK, Schuz A. 2012. Color blobs in cortical areas V1 and V2 of the new world monkey *Callithrix jacchus*, revealed by non-differential optical imaging. *J Neurosci.* 32:7881–7894.
- Victor JD, Purpura K, Katz E, Mao B. 1994. Population encoding of spatial frequency, orientation, and color in macaque V1. *J Neurophysiol.* 72:2151–2166.
- Weltzien F, Dimarco S, Protti DA, Daraio T, Martin PR, Grunert U. 2014. Characterization of secretagogin immunoreactive amacrine cells in marmoset retina. *J Comp Neurol.* 522:435–455.
- Wiesel TN, Hubel DH. 1966. Spatial and chromatic interactions in the lateral geniculate body of the rhesus monkey. *J Neurophysiol.* 29:1115–1156.
- Wikler KC, Rakic P. 1990. Distribution of photoreceptor subtypes in the retina of diurnal and nocturnal primates. *J Neurosci.* 10:3390–3401.
- Xiao Y, Casti A, Xiao J, Kaplan E. 2007. Hue maps in primate striate cortex. *Neuroimage.* 35:771–786.
- Xing D, Yeh CI, Shapley RM. 2009. Spatial spread of the local field potential and its laminar variation in visual cortex. *J Neurosci.* 29:11540–11549.
- Zaidi Q, Halevy D. 1993. Visual mechanisms that signal the direction of color changes. *Vision Res.* 33:1037–1051.